Diel Variability Affects the Inorganic Marine Carbon System in the Sea-Surface Microlayer of a Mediterranean coastal area (Šibenik, Croatia)

5   Ander López-Puertas[1,2], Oliver Wurl[1], Sanja Frka[3], Mariana Ribas-Ribas[1]

[1] Center for Marine Sensors (ZfMarS), Institute for Chemistry and Biology of the Marine Environment (ICBM), School of Mathematics and Science, Carl von Ossietzky Universität Oldenburg, Ammerländer Heerstraße 114-118, 26129 Oldenburg, Germany

[2] Instituto Universitario de Investigación Marina (INMAR), Universidad de Cádiz, 11510, Puerto Real, Cádiz,
10   Spain

[3] Laboratory for Marine and Atmospheric Biogeochemistry, Division for Marine and Environmental Research, Ruđer Bošković Institute, Bijenicka c. 54, 10000 Zagreb, Croatia

Correspondence to: Ander López-Puertas (ander.lopezpuertas@uca.es)

15   **Abstract**

The ocean plays a crucial role in the global carbon cycle by absorbing and storing substantial amounts of atmospheric carbon dioxide (CO_2). It is estimated that the ocean has sequestered approximately 26% of CO_2 emissions over the last decade, resulting in significant changes in the marine carbon system and impacting the marine environment. The sea-surface microlayer (SML) plays a crucial role in these processes, facilitating the
20   transfer of materials and energy between the ocean and the atmosphere. However, most studies on the carbon cycle in the SML have primarily addressed daily variability and overlooked nocturnal processes, which may lead to inaccurate global carbon estimates. We analysed temperature, salinity, pH_{T25}, and pCO_2 using data collected over three complete diel cycles during an oceanographic campaign along the Croatian coast near Šibenik in the Middle Adriatic. Our analysis revealed statistically significant differences ($p < 0.05$) between daytime and nighttime
25   measurements of temperature, salinity, and pH_{T25}. These differences may be related to the occurrence of buoyancy fluxes, which are typically more pronounced during the day and could enhance CO_2 fluxes, as observed with values of 1.98 ± 2.52 mmol cm^{-2} h^{-1} during the day, while at night, they dropped to 0.01 ± 0.02 mmol cm^{-2} h^{-1}. These findings emphasise the importance of considering complete diurnal cycles to accurately capture the variability in thermohaline features and carbon exchange processes, thereby improving our understanding of the role of the
30   ocean in climate change.

1.   Introduction

The ocean is a crucial climate regulator that mitigates the effects of anthropogenic emissions (Gattuso *et al*., 2015). It absorbs a significant portion of the Earth's excess heat (Hoegh-Guldberg *et al*., 2014) and captures a substantial amount of anthropogenic carbon dioxide (CO_2) emissions (Wong *et al*., 2014). It is well known that CO_2

35 significantly affects marine chemistry (Doney *et al*., 2009; Gattuso *et al*., 2015), and it is estimated that the ocean has sequestered approximately 26% of global CO_2 emissions in the last decade (Friedlingstein *et al*., 2024). Consequently, changes in the ocean environment have exceeded the magnitude and rate of natural variation due to anthropogenic carbon perturbation over the last millennia (Gattuso *et al*., 2015). In this context, the marine carbon system undergoes substantial modifications, resulting in various effects on the marine environment, including a

40 decrease in pH levels (Cantoni *et al*., 2012; Doney *et al*., 2009). Therefore, understanding the evolving state of marine biogeochemistry in the context of climate change is crucial, with a primary focus on the upper layers of the water column, which are closely linked to ocean-atmosphere interactions.

In the ocean-atmosphere system, the sea-surface microlayer (SML) plays a vital role in transferring materials and energy, such as heat, gases, and particles (Wurl *et al*., 2019), which must pass through it (Frka *et al*., 2009; Stolle

45 *et al*., 2020). The SML is a distinctive and complex marine environment that represents the interfacial boundary layer between the ocean and the atmosphere (Frka *et al*., 2009; Wurl *et al*., 2011). Its thickness typically does not exceed 1000 μm, and it exhibits distinct biological and physicochemical properties compared with the underlying water masses (Cunliffe *et al*., 2013; Stolle *et al*., 2020; Wurl *et al*., 2011). Thus, the SML experiences instantaneous meteorological forcing, such as solar radiation, wind, and atmospheric inputs (Wurl *et al*., 2019; Gassen *et al*.,

50 2023), which impacts the development of physical and biogeochemical processes occurring in the underlying water (Liss & Duce, 1997; Stolle *et al*., 2020). These characteristics of the SML overlap with the growing interest in oceanographic research to study the spatiotemporal variability of the marine carbon system (Cantoni *et al*., 2016), as this layer is essential for understanding global marine biogeochemistry. However, to gain a comprehensive spatiotemporal perspective on marine carbon chemistry processes, focusing on underexplored fields, such as the

55 role of nocturnal processes within the diel cycle, is crucial.

Daily variations force cyclic changes in chemistry (De Montety *et al*., 2011), which are influenced by processes such as photosynthesis, gas exchange between the ocean and atmosphere, and various environmental conditions (e.g., light, temperature, and nutrient availability) (Poulson & Sullivan, 2010). These processes directly affect the seawater pH by adding or removing CO_2 from seawater (Poulson & Sullivan, 2010; Takahashi *et al*., 2002). It is

60 well known that photosynthesis consumes CO_2 during the day, thereby reducing pCO_2 levels, and consequently causing an increase in pH (Cantoni *et al*., 2012; Takahashi *et al*., 2002). At night, the CO_2 produced by respiration tends to be more constant and accumulates in the water column, leading to an increase in pCO_2 and a decrease in pH (Cantoni *et al*., 2012). Although these processes are significant for seawater chemistry, research has predominantly focused on diurnal processes. As a result, the roles of respiration and other nocturnal processes in

65 the SML remain largely unexplored.

Within this framework, the Mediterranean Sea presents a unique research opportunity to investigate the spatiotemporal variability of the marine carbon system. It is often referred to as a "laboratory basin" (Bergamasco & Malanotte-Rizzoli, 2010; Robinson & Golnaraghi, 1994) because it allows us to approximate processes occurring on a global scale within a shorter time and space (Álvarez *et al*., 2014). Despite representing 0.8% of

70 the global ocean surface (Álvarez-Rodríguez, 2012), the Mediterranean Sea is considered an important anthropogenic carbon storage (Álvarez *et al*., 2014), as it absorbs a disproportionally larger amount of anthropogenic carbon compared to the global ocean (Hassoun *et al*., 2015; Schneider *et al*., 2010). Higher acidification ranges (-0.001 to -0.009 pH unit yr^{-1}) (Hassoun *et al*., 2022) were measured and exceeded those

measured in the Atlantic Ocean (-0.001 to -0.0026 pH unit yr^{-1}) (Takahashi *et al*., 2014). However, as explored in
75   this study, the dynamics of biogeochemical processes in coastal regions are more complex than those in the open
ocean (Borges, 2005). When examining oceanic regions, it is crucial to acknowledge that daily variability
profoundly affects marine carbon chemistry.

This study emphasises the role of diel variability in thermohaline features and dynamics of the marine inorganic
carbon cycle in the coastal region of the Mediterranean Sea (Šibenik, Croatia), thereby providing a comprehensive
80   understanding of the processes that influence the complete diurnal cycle. Therefore, it is essential to incorporate
nocturnal processes into global estimates of marine carbon cycle dynamics. We present high-resolution data to
understand biogeochemical processes and their variability in the water column, which complicates predictions of
coastal marine carbon system variations (Cantoni *et al*., 2012). We have focused on understanding the nocturnal
processes that affect the inorganic carbon system, thereby helping to clarify the uncertainties associated with this
85   system. This study contributes to the identification of anthropogenic influences on the marine environment in the
context of climate change.

2. Materials and Methods

2.1. Sampling Strategy and Seawater Analyses

Sampling was conducted in the Middle Adriatic region, specifically on the Croatian coast near Šibenik (Figure 1).
90   Temperature, conductivity, and pH data from the SML were collected using sensors integrated in a flow-through
system on the "Sea Surface Scanner (S^3)" (Ribas-Ribas *et al*., 2017) during a six-day campaign in August 2020
(from 10 to 15 August 2020). Measurements of the underlying water (ULW; ~1 m) were performed similarly. Solar
radiance and wind data were collected from a meteorological station (Davis Instruments, Vantage Pro2 Plus)
located on Zlarin Island. This study collected high-volume samples of approximately 15 L from the SML and ULW
95   for comprehensive analyses related to the SML. Discrete samples designated for the inorganic carbon parameters
were collected directly from the S^3 output and immediately sealed to prevent atmospheric contamination. These
measurements were conducted six times per diel cycle, each lasting 30–45 minutes, with a sampling frequency of
30 seconds. Three diurnal cycles were conducted during the study period. In each cycle, the first four
measurements were taken during periods of noticeable solar radiation (diurnal data), whereas the last two occurred
100   without solar radiation (nocturnal data).

Subsamples from the SML and ULW were collected in high-density polyethylene (HDPE) bottles to determine the
phosphate (PO$_4^{3-}$) and silicate [Si(OH)$_4$] concentrations. To preserve the samples, mercury chloride (HgCl$_2$) was
added. The preserved samples were stored at +4 °C until further analysis in the laboratory. Nutrient concentrations
were measured using a sequential automatic analyser (SAA, SYSTEA EASYCHEM) according to the standard
105   protocols described by Laskov *et al*., (2007) and Fanning & Pilson, (1973).
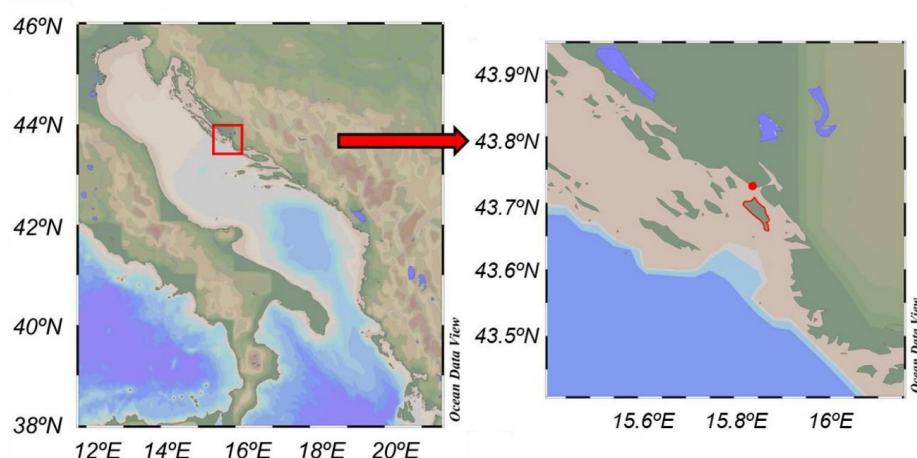
Figure 1. Map of the sampling area in the Middle Adriatic Sea, created using Ocean Data View (Schlitzer, 2022). The red dot indicates the sampling area, whereas Zlarin Island, where the meteorological station is situated, is outlined in red.

110

2.2. Marine Carbon System Determination

DIC samples (20 mL) were analysed by coulometric titration (CM 5014, UIC, USA) with an excess of 10% phosphoric acid. Total Alkalinity (TA) samples (100 mL) were measured via potentiometric titration (916 Ti-Touch, Metrohm, Switzerland) and calculated using a modified Gran plot approach implemented in Calkulate (version 1.8.0) (Humphreys *et al*., 2022). Calibration was performed with certified reference material (Batch 187) obtained from A. G. Dickson at the Scripps Institution of Oceanography. The 1σ measurement precision was ±3 μmol kg⁻¹ for DIC and ±2 μmol kg⁻¹ for TA.

To eliminate the effects of temperature variation on the results, the pH values measured in the seawater samples were adjusted to the average temperature value of 25.43 ºC, hereafter referred to as pH_{T25}. The normalisation utilised an adjustment factor of 0.018 pH units per °C, which is widely accepted for the range of pH and TA conditions typical of seawater (Eq. 1) (Dickson *et al*., 2007; Dickson & Millero, 1987; Zeebe & Wolf-Gladrow, 2001):

$$pH_{T25} = pH + (T - 25.43) \cdot 0.018 \qquad (1)$$

To evaluate the marine carbon system, the partial pressure of CO_2 (pCO_2) was calculated with the CO2SYS program (Version v3.2.0, MATLAB) (Sharp *et al*., 2020; Van Heuven *et al*., 2011) using as input parameters: DIC; TA, PO_4^{3-}, and $Si(OH)_4$; salinity (S); temperature (T), and pressure. The respective dissociation constants were used for carbon (Mehrbach *et al*., 1973), sulfate (KSO₄) (Dickson & Millero, 1987), fluorine (KF) (Perez & Fraga, 1987), and the borate-salinity ratio (Lee *et al*., 2010). Missing pCO_2 values were due to erroneous DIC and/or TA measurements. Consequently, standard deviations could not be calculated when the number of reliable data points was less than three. Once the pCO_2 values were calculated, the CO_2 flux through the ocean-atmosphere interface in the monitoring area was estimated using the following equation:

$$F = \Delta pCO_2 \cdot k \cdot \alpha \qquad (2)$$

where F is the CO_2 flux (mmol m^{-2} d^{-1}), ΔpCO_2 is equal to the difference in the partial pressures of the gas between the surface water and the atmosphere, k is the gas transfer coefficient (cm h^{-1}) from Wanninkhof, (2014), and α is the solubility of CO_2 in seawater (mol L^{-1} atm^{-1}). To calculate the partial pressure gradient of CO_2, atmospheric pCO_2 data were sourced from the Mauna Loa Observatory dataset of monthly means for August 2020 (Lan et al., 2023). The percentage error associated with excluding nocturnal fluxes in the daily average calculation was determined by comparing the mean fluxes calculated with and without nocturnal data, expressed as the relative difference between the two values.

To ensure high-quality data, a correction factor (CF) was applied to the continuous salinity and pH$_{T25}$ data. Discrete salinity values obtained from laboratory analyses served as reference points and were compared to the average continuous values recorded by the S^3 (Ribas-Ribas *et al*., 2017). This process resulted in the derivation of distinct CFs, which were applied at each depth and during each time interval of the S^3 measurements (Ribas-Ribas et al., 2017). Once the salinity values were corrected, the pH was calculated using the CO2Sys program (Version v3.2.0, MATLAB) (Sharp *et al*., 2020; Van Heuven *et al*., 2011). These calculated pH$_{T25}$ values were then utilised as reference points for comparison with the average continuous values obtained from the S^3 measurements (Ribas-Ribas et al., 2017). After correcting for salinity, the density (ρ) was calculated using the TEOS-10 (https://www.teos-10.org/index.htm) equation of state in RStudio based on the observed temperature and salinity values. From this calculation, sigma-*t* was defined as the density at a given temperature and salinity minus 1,000 kg m^{-3}.

2.3. Evaporation rate calculation

The evaporation rate (E) (Gill, 1982) was estimated using the following formula, which relates the latent heat flux (Q$_E$) (Brutsaert, 2013), the latent heat of vaporisation (Lv) (Kittel & Kroemer, 1980), and the calculated density of seawater (ρ):

$$E = \frac{Q_E}{Lv \cdot \rho} \qquad (3)$$

2.4. Statistical Analysis

Since the assumptions of normality and homoscedasticity were not met for the collected data, the Kruskal-Wallis test was chosen as a nonparametric alternative to ANOVA. This test identified significant differences between the data collected during the day and night, between the SML and ULW, and among the medians of the cycles studied. A significance level (α) of 0.05 was established to determine whether the groups differed significantly. All statistical analyses were performed using RStudio. In addition, to carry out a complete analysis of the variability of the marine carbon system during the study period, the anomalies in temperature, salinity, pH$_{T25}$, and pCO_2 data were calculated using the following expression: Δ (SML – ULW). These differences were calculated for diurnal and nocturnal data for each cycle.

3. Results

The primary objective of this study was to understand the global patterns of diurnal variability and depth-related differences in marine biogeochemistry during the observed cycles. Temperature, salinity, pH$_{T25}$, and pCO_2 were

used to perform a statistical analysis of the similarity between the data collected during the diel cycle and to calculate the differences between the values measured in the SML and ULW. Additionally, we examined the temporal distribution using box-and-whisker plots and calculated the air-sea CO_2 exchange across the SML.

3.1. Meteorological conditions

To study the potential variance in the meteorological forcing observed during the observations, time-series graphs were plotted for solar radiation and wind speed (Figure 2). A consistent pattern of solar radiation was observed during all three cycles, with peaks of 525, 404, and 420 W m^{-2} observed at 14:00 UTC. Relatively low wind speeds were recorded during the day in all three cycles, averaging 1.26 ± 1.46 m s^{-1}. Maximum wind speeds were observed at 14:00 and 18:00 UTC, higher for Cycles 1 and 2 (2.14 m s^{-1} and 5.22 m s^{-1}) than during Cycle 3 (0.95 m s^{-1}). Additionally, a decrease in wind speed was observed throughout the night, approaching near-zero values, except during Cycle 3 when the wind speed remained consistently close to zero.
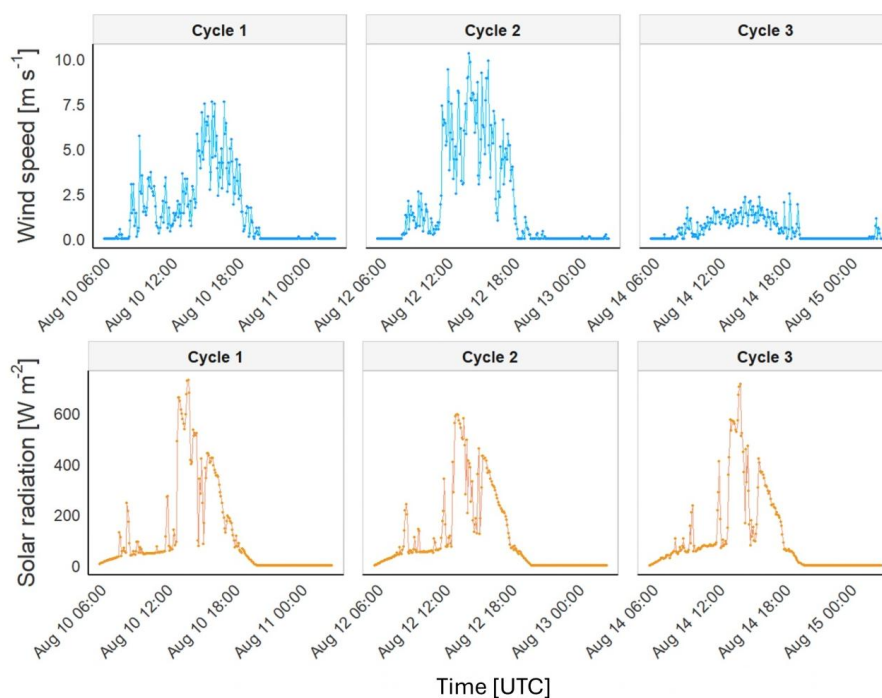
Figure 2. Time series showing wind speed and solar radiation on Zlarin Island (Figure 1) during the three studied cycles.

3.2. Daily trends

To investigate the overall distribution of physicochemical parameters throughout the daily sampling period at SML and ULW, we show box-and-whisker plots for temperature, salinity, and pH$_{T25}$ across different time intervals (Figure 3). We also performed the Kruskal-Wallis test to determine statistically significant differences between the SML and ULW (Table S1). The analysis revealed no significant temperature differences between the two depths during Cycle 1 (SML: 25.00 ± 0.85 ºC; ULW: 24.90 ± 0.72 ºC) and Cycle 2 (SML: 25.40 ± 0.62 ºC; ULW: 25.40

185 ± 0.83 ºC). However, in Cycle 3, ULW was slightly warmer, with a mean temperature of 26.60 ± 0.72 °C compared to 26.20 ± 1.20 °C in the SML. For salinity, significant differences were detected between SML and ULW during Cycles 1 and 2, with ULW exhibiting higher salinity levels in Cycle 1 (SML: 38.90 ± 0.32 g kg^{-1}; ULW: 39.10 ± 0.32 g kg^{-1}) and in Cycle 2 (SML: 39.2 ± 0.27 g kg^{-1}; ULW: 39.4 ± 0.29 g kg^{-1}). Notably, the salinity data showed greater variability, especially in Cycle 2, in the SML, whereas the ULW remained relatively constant. The

190 pH_{T25} data collected over the three cycles displayed considerable variability, with fluctuations observed throughout the day. The SML and ULW data showed significant differences during the first two cycles, with slightly higher values in the SML for Cycle 1 (SML: 8.030 ± 0.020; ULW: 8.020 ± 0.033) and for Cycle 2 (SML: 8.020 ± 0.020; ULW: 8.010 ± 0.024). No significant differences were observed in Cycle 3 (SML: 8.020 ± 0.032; ULW: 8.020 ± 0.032).
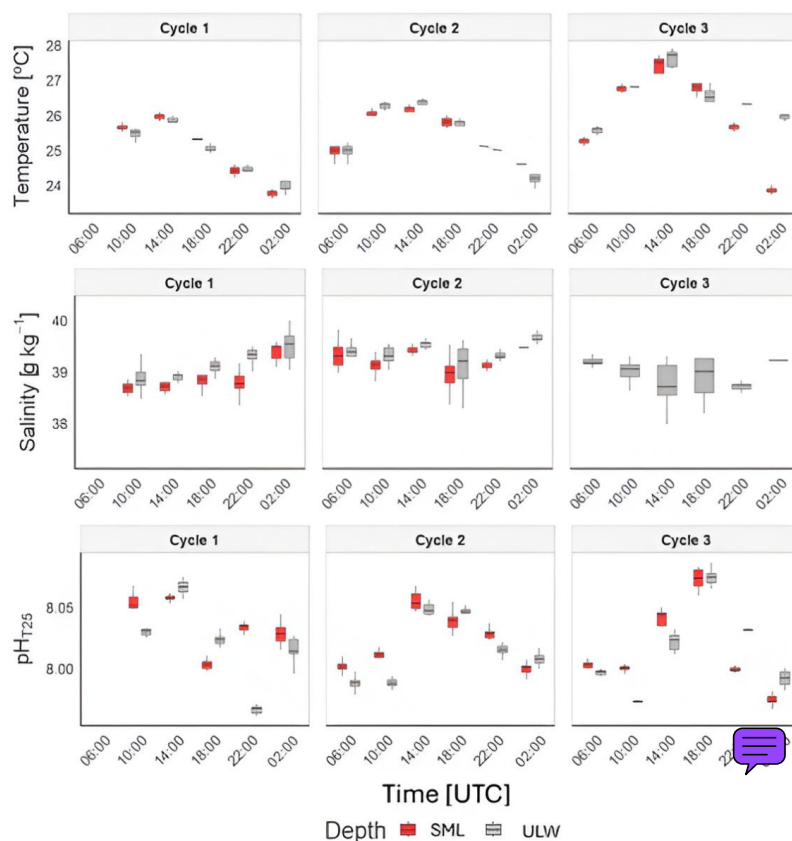
195

Figure 3. Box-and-whisker plots for the different time steps at which measurements were obtained at both the SML and ULW for temperature, salinity, and pH$_{T25}$. The horizontal line within each box denotes the mean of the data, whereas the vertical line associated with each box represents the 25th and 75th percentiles (Q1 and Q3) of the data.

3.3. Diel variability and depth-related anomalies

To assess diel variability in the marine carbon system, we statistically compared the thermohaline and key carbon cycle variables, pH_{T25} and pCO_2, between day and night in the SML and ULW (Figure 4, Table 1). Additionally, we calculated ΔSML-ULW to evaluate the magnitude of vertical anomalies during diurnal and nocturnal conditions. The analysis of thermohaline variables indicated significant differences between diurnal and nocturnal data at the two depths across the three cycles (Table S2). However, the salinity data from ULW during Cycle 3 did not exhibit significant differences. The observed anomalies between the SML and ULW varied across the three cycles for temperature (Table 1). In Cycle 1, the SML exhibited positive temperature anomalies during the day and negative anomalies at night (Table 1). In contrast, Cycle 2 showed negative diurnal and positive nocturnal temperature anomalies. During Cycle 3, both diurnal and nocturnal temperature anomalies in the SML were negative. Similarly, salinity anomalies in the SML were consistently negative in Cycles 1 and 2 for both day and night measurements (Table 1). These patterns indicate that external forcing may modulate thermohaline properties, contributing to the marked temporal variability observed across the diel cycle.
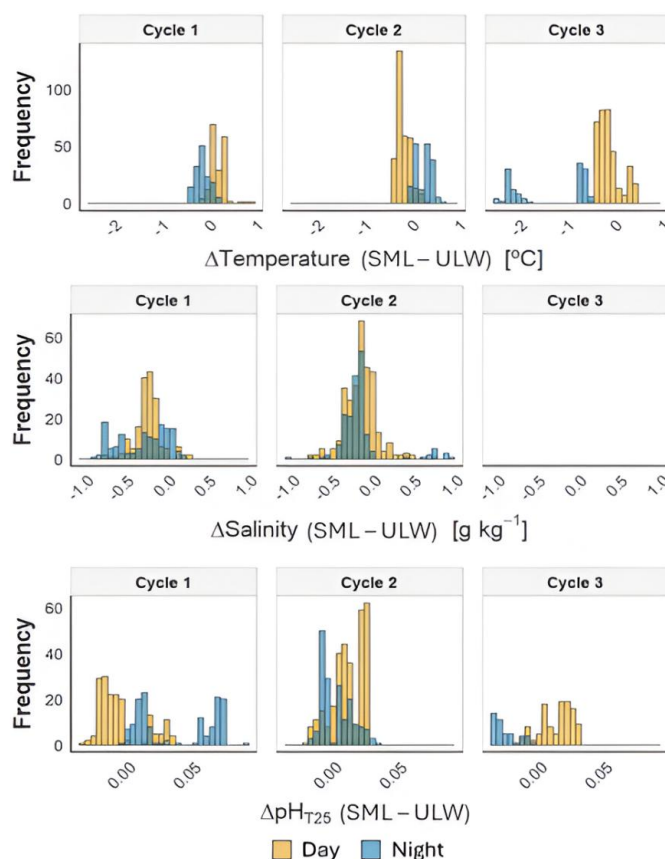
Figure 4. Frequency distribution of temperature, salinity, and pH$_{T25}$ differences between SML and ULW observed during the day (orange) and at night (blue) across the three cycles studied.

When comparing the diurnal and nocturnal data for the variables associated with the marine carbon system at each depth (Table S2), we found significant differences in pH_{T25}, except for the ULW data during Cycle 3. However, no significant differences were observed in the pCO_2 data. The pH_{T25} deltas (Table 1) revealed that during Cycle 1, lower pH_{T25} values were recorded in the SML for diurnal data and higher for nocturnal data (-0.006 ± 0.018; 0.038

220 ± 0.029). During Cycle 2, the SML showed higher diurnal (0.011 ± 0.012) and lower nocturnal (-0.002 ± 0.012) pH_{T25} values. Meanwhile, for Cycle 3, the SML indicated higher pH_{T25} values for the diurnal data (0.013 ± 0.012) and lower values for the nocturnal data (0.026 ± 0.009) (Table 1). For the pCO_2 data during Cycles 1 and 3, lower pCO_2 values were recorded in the SML during both diurnal (-11 ± 56 µatm and -22 ± 22 µatm, respectively) and nocturnal periods (-4 and -8 µatm, respectively) (Table 1). In Cycle 2, lower diurnal and higher nocturnal values

225 were observed in the SML, with values of -12 ± 19 µatm and 7 µatm, respectively. The large variability between the nighttime and daytime data distributions at the two depths can be attributed to the complex interaction between biological processes and atmospheric and oceanic forcing, such as heat flux and mixing processes.

Table 1. Mean anomalies of temperature, salinity, pH_{T25}, and pCO_2 between the two depths studied (Δ(SML-ULW)).

		Temperature [ºC]		Salinity [g kg^{-1}]		pH_{T25}		pCO_2 [µatm]	
		n	Δ SML-ULW	n	Δ SML-ULW	n	Δ SML-ULW	n	Δ SML-ULW
Cycle 1	Day	177	0.19 ± 0.14	606	-0.23 ± 0.17	175	-0.006 ± 0.018	3	-11 ± 56
	Nigth	142	-0.10 ± 0.14	426	-0.29 ± 0.30	140	0.038 ± 0.029	1	-4
Cycle 2	Day	312	-0.13 ± 0.12	972	-0.14 ± 0.19	324	0.011 ± 0.012	4	-12 ± 19
	Nigth	180	0.28 ± 0.18	559	-0.15 ± 0.29	184	-0.002 ± 0.012	2	7
Cycle 3	Day	365	-0.08 ± 0.24	-	-	141	0.013 ± 0.012	4	-22 ± 22
	Nigth	132	-1.34 ± 0.77	-	-	53	-0.026 ± 0.009	2	-8

230

3.4. Biogeochemical processes variability across diel cycles

To assess the variability of biogeochemical processes during the diel cycle, we present time series of temperature, salinity, and pH_{T25} (Figure 5). In the time series, large fluctuations were primarily observed in the SML, particularly during the day. This increased variability is consistent with the patterns described in the previous section, although

235 the standard deviations between SML and ULW are similar overall (Table S2). The changes during the day occurred rapidly, with increases and decreases spanning 3- 5-minute intervals for the three parameters. More specifically, during sampling at 18:00 UTC of Cycle 2, we recorded variations over brief intervals, specifically showing changes of approximately 0.28 °C in temperature, 0.30 g kg^{-1} in salinity, and 0.016 units in pH_{T25}. During the night, fluctuations were less frequent and of smaller magnitude, except for a sudden change at the end of the

240 sampling conducted at 02:00 UTC in Cycle 2. At that point, there was a slight increase in pH_{T25} at both SML and ULW, along with a decrease in salinity at both depths. This observation suggests that daytime surface heating,

evaporation, and production processes likely result in changes in temperature, salinity, and pH$_{T25}$, which are less pronounced at night.
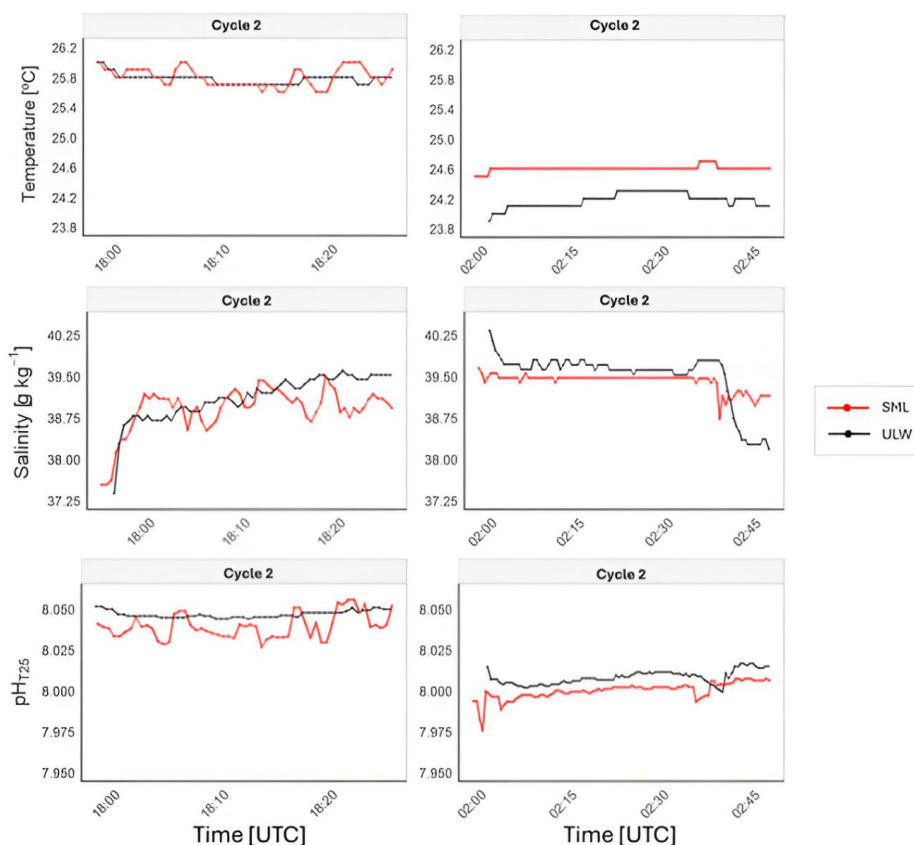
Figure 5. Time series data of temperature, salinity, and pH$_{T25}$ collected during Cycle 2: Diurnal (18:00 UTC, August 12) and Nocturnal (02:00 UTC, August 13) measurements.

To assess the variability observed in the SML, the sigma-*t* time series for Cycle 2 at 18:00 UTC and 02:00 UTC was plotted (Figure 6), and evaporation rates within the SML were calculated for Cycles 1 and 2 (Table 2), as salinity data required for calculations in Cycle 3 were not available. The sigma-*t* time series throughout the day exhibits greater variability in the SML compared to nocturnal data, when the density fluctuation decreased. However, this variability trend was not observed in the ULW. The observed patterns of temperature, salinity, pH$_{T25}$, and sigma-*t* align with the calculated evaporation rates. In Cycles 1 and 2, the evaporation rates peaked at 14:00 UTC (0.043 mm h^{-1} and 0.074 mm h^{-1}, respectively). They remained high during the late afternoon at 18:00 UTC (0.042 mm h^{-1} and 0.041 mm h^{-1}, respectively), coinciding with the periods of highest solar radiation and wind speed (Figure 2). In contrast, the evaporation rate was close to zero at night. This behaviour highlights the

influence of meteorological forcing on the SML during the day, highlighting the connection between evaporation and the variability observed.
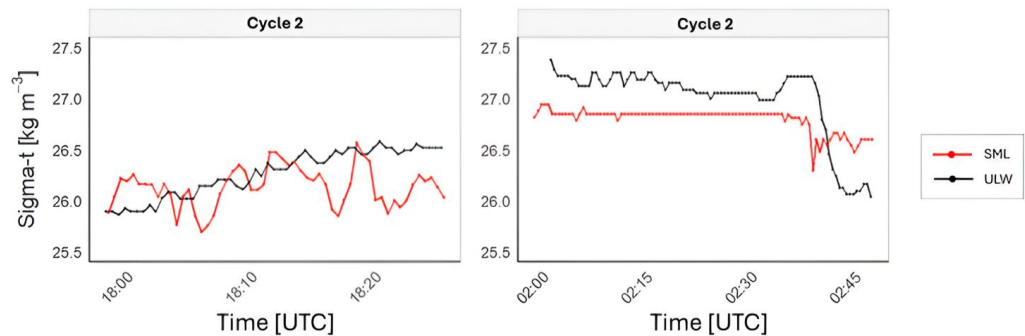
Figure 6. Time series during Cycle 2 for diurnal (18:00 UTC on August 12) and nocturnal (02:00 UTC on August 13) sigma–t data. Sigma-t is defined as the density at a given temperature and salinity minus 1,000 kg m⁻³.

Table 2. Estimated evaporation rates (mm h⁻¹) based on latent heat flux and seawater density in the SML.

	Evaporation rates [mm h^{-1}]			
Cycle	Time (UTC)	Mean	sd	n
Cycle 1	06:00			
	10:00	0.031	$1.261 \cdot 10^{-3}$	41
	14:00	0.043	$4.646 \cdot 10^{-4}$	67
	18:00	0.042	$6.674 \cdot 10^{-4}$	64
	22:00	0.000	0.00	66
	02:00	0.000	0.00	76
Cycle 2	06:00	0.000	0.00	68
	10:00	0.012	$2.040 \ 10^{-4}$	111
	14:00	0.074	$1.667 \cdot 10^{-3}$	78
	18:00	0.041	$8.670 \cdot 10^{-4}$	55
	22:00	0.000	0.00	82
	02:00	0.000	$3.960 \cdot 10^{-6}$	98

To study the gas exchange between the atmosphere and the ocean, we calculated the CO_2 fluxes and k values using a wind-based parameterisation (Wanninkhof, 2014) for all three cycles and during both day and night (Figure 7). In Cycle 1, despite the incomplete data, a flux of 3.68 ± 1.16 mmol cm⁻² h⁻¹ was detected during the day, while the flux was close to zero at night. A similar pattern appeared in Cycles 2 and 3, where the fluxes peaked at approximately 14:00 UTC and declined to near zero thereafter. However, the mean flux was higher in Cycle 2

270    $(2.11 \pm 3.31 \text{ mmol cm}^{-2} \text{ h}^{-1})$ than in Cycle 3 $(0.22 \pm 0.28 \text{ mmol cm}^{-2} \text{ h}^{-1})$, consistent with stronger winds. The average wind speeds during the day were 1.5, 1.9, and 0.4 m s^{-1} for each cycle, respectively, while at night, winds dropped to nearly 0 m s^{-1} in the three cycles. The k values during the day were 1.12 ± 0.15, 2.22 ± 3.31, and 0.09 ± 0.11 cm h^{-1}, whereas at night, they were close to 0 cm h^{-1}. In this context, excluding nocturnal fluxes in the daily average calculations introduced local percentage errors of 33%, 50%, and 43% for Cycles 1, 2, and 3, respectively.

275   The increased daytime wind speeds enhanced CO_2 fluxes, whereas calm nighttime conditions were associated with reduced or nearly zero gas transfer velocities.
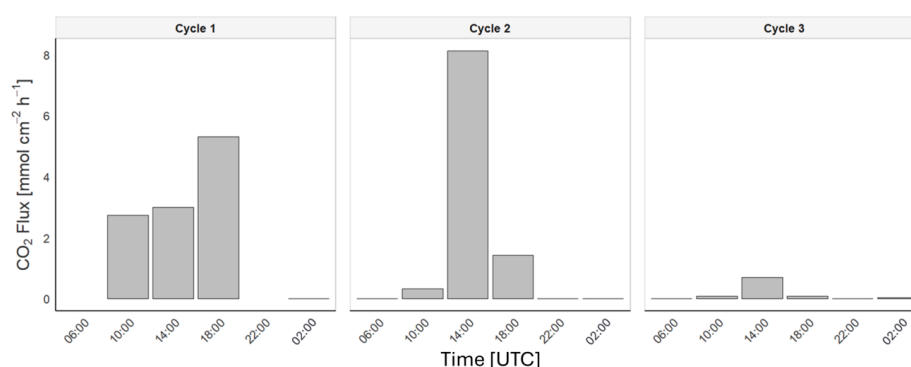
Figure 7. CO_2 fluxes between the atmosphere and the ocean during the studied cycles.

280   **4. Discussion**

This study revealed high variability in the SML and ULW during the diel cycle, with significant differences ($p < 0.05$) in temperature, salinity, and pH_{T25} when comparing diurnal and nocturnal data at both depths (Table S1). These results highlight the differences between the meteorological forces that influence the physicochemical properties of seawater during the day and night. For example, during the day, the combined forcing of solar radiation and increased wind speed enhances evaporation rates (Table 2), resulting in the cooling of the SML

285   (Gassen *et al*., 2023), thus causing changes in temperature, salinity, and pH_{T25} (Figure 4). This means that the SML is subjected to short-time fluctuations that coincide with changes in wind speed. These fluctuations directly influence thermohaline features, CO_2 system parameters (Acuña et al., 2008), and the kinetics of the metabolic processes occurring in the marine environment (Nimick *et al*., 2011). Accordingly, in response to the solar photocycle, many marine biogeochemical processes operate on a 24-hour cycle (Nimick *et al*., 2011), with daily

290   variations comparable in magnitude to the annual variations associated with the amount of solar radiation reaching the ocean surface at different times of the year (Herring *et al*., 1990; Nimick *et al*., 2011).

Regarding the variability observed during the day and night, we detected differences in the diurnal temperature data, reaching up to +1.89 ºC in the SML and +1.36 ºC in the ULW. The calculated mean temperature values

295   correspond to the Middle Adriatic Surface Water mass (Table S1). Previous studies have reported mean summertime temperatures in the SML of 25.1 ºC (Frka *et al*., 2009) and 27.4 ± 2.9 ºC (Milinković *et al*., 2022). Interestingly, the negative diurnal SML anomalies in Cycles 2 and 3 differ from the typical warming pattern in low

wind conditions (Wurl *et al*., 2019), suggesting that localized mixing or evaporative cooling may have offset surface warming. Similarly, the observed negative salinity anomaly in the SML could also be linked to these

300   processes. While evaporation driven by intense solar radiation tends to increase salinity in the SML (Frka *et al*., 2009; Wurl *et al*., 2019), the consistently negative salinity anomalies observed in Cycles 1 and 2 (Table 1) suggest vertical mixing. This explains the daily variability in salinity distribution between the SML and ULW, with mean values of 39.09 ± 0.33 g kg^{-1} and 39.15 ± 0.34 g kg^{-1}, respectively. The Krka River has the highest outflow rates in the region, but it usually has lower discharge during the summer months, which contributes to the increased

305   salinity observed in the SML and ULW (Frka *et al*., 2009; Marcinek *et al*., 2020). During dry periods, submarine groundwater discharge contributes only a small amount, between 0.19-0.31 m³ s^{-1} (Liu et al., 2019), compared to its annual mean of 52.9 m³ s^{-1} (Bužančić *et al., 2016*; Marcinek *et al.*, 2020).

The interaction between biological processes and the physicochemical properties of seawater is complex (Álvarez *et al*., 2014; Cantoni *et al*., 2012) and has a delicate balance in the marine environment (Cantoni *et al*., 2012;

310   Takahashi *et al*., 2002). This interaction directly influences biogeochemical processes typically regulated by production and respiration (Poulson & Sullivan, 2010). These processes significantly affect the pH of seawater through the uptake or removal of CO_2. During the day, photosynthesis lowers pCO_2 levels and increases pH by consuming CO_2, whereas at night, CO_2 from respiration accumulates, increasing pCO_2 and decreasing pH (Cantoni *et al*., 2012). However, as we can see in Cycle 3 (Table S2), the observed increase in pCO_2 (525 ± 47 µatm) and

315   pH$_{T25}$ (8.042 ± 0.020) values during the day compared to those measured at night (465 µatm; 7.993 ± 0.026) may be linked to several processes, including increased respiration and various environmental factors that may offset the anticipated effects of photosynthesis or the possibility of photoinhibition caused by excessive solar radiation (Feng *et al*., 2008), and an accumulation of CO_2 in the upper layers of the water due to limited mixing (Takahashi *et al*., 2002).

320   The complexity of the coupled thermohaline and pH dynamics in seawater is highlighted in the time-series results (Figure 5). The observed fluctuations in the SML for temperature, salinity, and pH$_{T25}$ may be due to buoyancy fluxes. Wind, thermohaline fluctuations, precipitation, and evaporation significantly influence the surface turbulence (Cronin & Sprintall, 2001). The SML absorbs heat from sunlight and cools through radiation and heat loss, leading to changes in temperature and salinity that disrupt buoyancy, cause convective overturning, entrain

325   deeper water from the ULW, and eventually promote mixing (Cronin & Sprintall, 2001). Wind can also enhance this process by creating tangential stress that acts as a vertical momentum flux. Temperature and salinity changes in the SML led to stratification or convection with mixing (Figure 5), depending on oceanic and atmospheric forcing. This process has already been observed in the SML (Wurl *et al*., 2019) and was found to regulate buoyancy fluxes through evaporative salinisation, playing a crucial role in the exchange of climate-relevant gases and heat

330   between the ocean and the atmosphere.

In this context, the existence of these buoyancy fluxes only during the day could also explain the diel difference in CO_2 exchange between the atmosphere and the ocean. As observed in this study, the CO_2 fluxes exhibited differences between daytime (1.98 ± 2.52 mmol cm^{-2} h^{-1}) and nighttime (0.01 ± 0.02 mmol cm^{-2} h^{-1}) conditions. Thus, during the day, buoyancy fluxes facilitate the exchange of CO_2 between the two compartments, accounting

335   for a higher flux than at night. Additionally, the absence of wind at night reduced the calculated flux to nearly zero, suggesting that gas transfer velocity parameterisations without an intercept may not be appropriate (Ribas-Ribas

et al., 2019). Moreover, even without wind, convective airflow driven by temperature gradients can facilitate gas exchange between the surface and atmosphere (Liss & Merlivat, 1986). This study's diel variability aligns with other research findings, suggesting that another main factor affecting this difference is the vertical pCO$_2$ gradient

340   in the upper water column, potentially affecting gas transfer estimates (Stolle *et al*., 2020). Therefore, neglecting nocturnal fluxes may result in overestimation, as in this study, where the three cycles were overvalued by 33%, 50%, and 44%, respectively.

5. Conclusions

This study observed a clear diel variability in the distribution of thermohaline features and variables describing

345   the marine inorganic carbon cycle, including temperature, salinity, pH$_{T25}$, and pCO$_2$. The SML experiences pronounced fluctuations in these parameters throughout the day, influenced by daily changes, like solar radiation, which directly affect the described variables and the environment's metabolic activity. In addition, higher CO$_2$ fluxes were observed during the day, coinciding with increased wind speeds and buoyancy fluxes that enhanced the CO$_2$ exchange between the two compartments. Thus, by emphasising the study of diel cycles, it has been

350   observed that the daily variability of biogeochemical processes is in a delicate balance, making it challenging to obtain a comprehensive global understanding of marine chemistry. Technological advances have been made in sampling equipment for short temporal and spatial scales in recent decades. However, such progress has not been extended to nighttime observations, which remain significantly more challenging due to greater logistical complexity and heightened safety considerations when operating aboard oceanographic vessels at night. In this

355   context, it is essential to study complete diel cycles, which are crucial for understanding the global carbon budget and its associated uncertainties. Thus, generating a network of diurnal cycle data will identify the drivers of changes in marine chemistry, allowing for assessing the responses of marine ecosystems in the context of climate change.

360   **Data Availability Statements**

The data supporting the findings of this study have been submitted to PANGAEA and are currently undergoing curation and DOI assignment. In the meantime, the data are available for review and use at https://cloud.uol.de/s/mKHmN3K8MqPnizg.

365   **Acknowledgements**

This work was funded by the German Research Foundation (DFG), project number 427614800, and by the Croatian Science Foundation under the project IP-2018-01-3105: *Biochemical Responses of Oligotrophic Adriatic Surface Ecosystems to Atmospheric Deposition Inputs* (BiREADI). It was also supported by the German Academic Exchange Service (DAAD) under project 57513644: *Diurnal Dynamics at the Sea-Atmosphere Interface (INSIST)*.

370   Additionally, the author gratefully acknowledges the support from the Erasmus + KA 131 SMP OUT program (2022-2023) for funding a research internship at the Carl von Ossietzky Universität Oldenburg - Institut für Chemie und Biologie des Meeres (ICBM). The authors thank Carola Lehners, Brandy T. Robinson, and Lisa Gassen for

operating the sea surface scanner and conducting SML sampling, Carmen Cohr for initial S[3] data treatment, and
Leonie Jaeger for assistance with the evaporation rate calculations.

375 **Author Contribution**

AL-P: Data Curation, Formal Analysis, Methodology, Visualization, Writing – Original Draft, Writing – Review
& Editing. **OW**: Funding Acquisition, Resources, Formal Analysis, Writing – Review & Editing. **SF**: Funding
Acquisition, Resources, Formal Analysis, Writing – Review & Editing. **MR-R**: Conceptualization, Formal
Analysis, Visualization, Funding Acquisition, Resources, Supervision, Writing – Original Draft, Writing – Review
380 & Editing.

References

Acuña, V., Wolf, A., Uehlinger, U., and Tockner, K.: Temperature dependence of stream benthic respiration in an
alpine river network under global warming, Freshw. Biol., 53, 2076–2088, https://doi.org/10.1111/j.1365-
385 2427.2008.02028.x, 2008.

Álvarez, M., Sanleón-Bartolomé, H., Tanhua, T., Mintrop, L., Luchetta, A., Cantoni, C., Schroeder, K., and
Civitarese, G.: The CO_2 system in the Mediterranean Sea: a basin wide perspective, Ocean Sci., 10, 69–
92, https://doi.org/10.5194/os-10-69-2014, 2014.

Álvarez-Rodríguez, M.: The CO_2 system observations in the Mediterranean Sea: past, present and future, in:
390 Designing Med-SHIP: a program for repeated oceanographic surveys, CIESM Workshop Monographs,
No. 43, edited by: Briand, F., CIESM, Monaco, pp. 41–50,
https://ciesm.org/catalog/index.php?article=1043, 2012.

Bergamasco, A., and Malanotte-Rizzoli, P.: The circulation of the Mediterranean Sea: a historical review of
experimental investigations, Adv. Oceanogr. Limnol., 1, 11–28,
395 https://doi.org/10.1080/19475721.2010.491656, 2010.

Borges, A. V.: Do we have enough pieces of the jigsaw to integrate CO_2 fluxes in the coastal ocean?, Estuaries, 28,
3–27, https://doi.org/10.1007/BF02732750, 2005.

Brutsaert, W.: Evaporation into the Atmosphere: Theory, History and Applications, Environmental Fluid
Mechanics, Springer, Dordrecht, Netherlands, 302 pp., https://doi.org/10.1007/978-94-017-1497-6, 2013.

400 Bužančić, M., Gladan, Ž. N., Marasović, I., Kušpilić, G., and Grbec, B.: Eutrophication influence on phytoplankton
community composition in three bays on the eastern Adriatic coast, Oceanologia, 58, 302–316,
https://doi.org/10.1016/j.oceano.2016.05.003, 2016.

Cantoni, C., Luchetta, A., Celio, M., Cozzi, S., Raicich, F., and Catalano, G.: Carbonate system variability in the Gulf of Trieste (North Adriatic Sea), Estuarine, Coastal Shelf Sci., 115, 51–62,

405   https://doi.org/10.1016/j.ecss.2012.07.006, 2012.

Cantoni, C., Luchetta, A., Chiggiato, J., Cozzi, S., Schroeder, K., and Langone, L.: Dense water flow and carbonate system in the southern Adriatic: A focus on the 2012 event, Mar. Geol., 375, 15–27, https://doi.org/10.1016/j.margeo.2015.08.013, 2016.

Cronin, M. F., and Sprintall, J.: Wind-and buoyancy-forced upper ocean, in: Elements of Physical Oceanography:

410   A Derivative of the Encyclopedia of Ocean Sciences, 237–245, https://doi.org/10.1006/rwos.2001.0157, 2001.

Cunliffe, M., Engel, A., Frka, S., Gašparović, B., Guitart, C., Murrell, J. C., Salter, M., Stolle, C., Upstill-Goddard, R., and Wurl, O.: Sea surface microlayers: A unified physicochemical and biological perspective of the air–ocean interface, Prog. Oceanogr., 109, 104–116, https://doi.org/10.1016/j.pocean.2012.08.004, 2013.

415 De Montety, V., Martin, J. B., Cohen, M. J., Foster, C., and Kurz, M. J.: Influence of diel biogeochemical cycles on carbonate equilibrium in a karst river, Chem. Geol., 283(1–2), 31–43, https://doi.org/10.1016/j.chemgeo.2010.12.025, 2011.

Dickson, A. G., and Millero, F. J.: A comparison of the equilibrium constants for the dissociation of carbonic acid in seawater media, Deep Sea Res. Part A, 34(10), 1733–1743, https://doi.org/10.1016/0198-

420   0149(87)90021-5, 1987.

Dickson, A. G., Sabine, C. L., and Christian, J. R. (Eds.): Guide to best practices for ocean CO_2 measurements, PICES Special Publication 3, North Pacific Marine Science Organization, 191 pp., ISBN 1-897176-07-4, 2007.

Doney, S. C., Fabry, V. J., Feely, R. A., and Kleypas, J. A.: Ocean Acidification: The Other CO_2 Problem, Annu.

425   Rev. Mar. Sci., 1(1), 169–192, https://doi.org/10.1146/annurev.marine.010908.163834, 2009.

Fanning, K. A., and Pilson, M.: On the Spectrophotometric determination of dissolved silica in natural waters, Anal. Chem., 45(1), 136–140, https://doi.org/10.1021/ac60323a021, 1973.

Feng, Y., Warner, M. E., Zhang, Y., Sun, J., Fu, F.-X., Rose, J. M., and Hutchins, D. A.: Interactive effects of increased pCO$_2$, temperature and irradiance on the marine coccolithophore Emiliania huxleyi

430   (Prymnesiophyceae), Eur. J. Phycol., 43(1), 87–98, https://doi.org/10.1080/09670260701664674, 2008.

Friedlingstein, P., O'Sullivan, M., Jones, M. W., Andrew, R. M., Hauck, J., Landschützer, P., Le Quéré, C., Li, H., Luijkx, I. T., and Olsen, A.: Global carbon budget 2024, Earth Syst. Sci. Data, 17, 965–1098, https://doi.org/10.5194/essd-17-965-2025, 2024.

Frka, S., Kozarac, Z., and Ćosović, B.: Characterization and seasonal variations of surface active substances in the

435   natural sea surface micro-layers of the coastal Middle Adriatic stations, Estuar. Coast. Shelf Sci., 85(4), 555–564, https://doi.org/10.1016/j.ecss.2009.09.023, 2009.

Gassen, L., Badewien, T. H., Ewald, J., Ribas-Ribas, M., and Wurl, O.: Temperature and Salinity Anomalies in the Sea Surface Microlayer of the South Pacific during Precipitation Events, J. Geophys. Res. Oceans, e2023JC019638, https://doi.org/10.1029/2023JC019638, 2023.

440   Gattuso, J.-P., Magnan, A., Billé, R., Cheung, W. W. L., Howes, E. L., Joos, F., … and Turley, C..: Contrasting futures for ocean and society from different anthropogenic CO_2 emissions scenarios, Science, 349(6243), aac4722, https://doi.org/10.1126/science.aac4722, 2015.

Gill, A. E.: Atmosphere-Ocean Dynamics, Academic Press, ISBN 0-12-283520-4, 1982.

Hassoun, A. E. R., Bantelman, A., Canu, D., Comeau, S., Galdies, C., Gattuso, J.-P., Giani, M., Grelaud, M.,

445   Hendriks, I. E., Ibello, V., Idrissi, M., Krasakopoulou, E., Shaltout, N., Solidoro, C., Swarzenski, P. W., & Ziveri, P.: Ocean acidification research in the Mediterranean Sea: Status, trends and next steps, Front. Mar. Sci., 9, 892670, https://doi.org/10.3389/fmars.2022.892670, 2022.

Hassoun, A. E. R., Gemayel, E., Krasakopoulou, E., Goyet, C., Abboud-Abi Saab, M., Guglielmi, V., Touratier, F., & Falco, C.: Acidification of the Mediterranean Sea from anthropogenic carbon penetration, Deep Sea

450   Res. Part I, 102, 1–15, https://doi.org/10.1016/j.dsr.2015.04.005, 2015.

Herring, P. J., Campbell, A. K., Whitfield, M., and Maddock, L. (Eds.): Light and Life in the Sea, Cambridge University Press, Cambridge, UK, 366 pp., ISBN 978-0521392075, 1990.

Hoegh-Guldberg, O., Cai, R., Poloczanska, E. S., Brewer, P. G., Sundby, S., Hilmi, K., Fabry, V. J., and Jung, S.: The ocean, in: Climate Change 2014: Impacts, Adaptation, and Vulnerability. Part B: Regional Aspects,

455   edited by: Barros, V. R., Field, C. B., Dokken, D. J., Mastrandrea, M. D., Mach, K. J., Bilir, T. E., Chatterjee, M., Ebi, K. L., Estrada, Y. O., Genova, R. C., Girma, B., Kissel, E. S., Levy, A. N., MacCracken, S., Mastrandrea, P. R., and White, L. L., Cambridge University Press, Cambridge, United Kingdom and New York, NY, USA, 1655–1731, https://doi.org/10.1017/CBO9781107415386.026, 2014.

Humphreys, M. P., Lewis, E. R., Sharp, J. D., and Pierrot, D.: PyCO2SYS v1.8: Marine carbonate system calculations in Python, Geoscientific Model Development, 15(1), 15–43, https://doi.org/10.5194/gmd-15-15-2022, 2022.

Kittel, C., and Kroemer, H.: Thermal Physics, Macmillan, ISBN 978-0716710882, 1980.

Lan, X., Tans, P., Thoning, K., and NOAA Global Monitoring Laboratory: Trends in globally-averaged CO_2 determined from NOAA Global Monitoring Laboratory measurements, NOAA GML [data set], https://doi.org/10.15138/9N0H-ZH07, 2023.

Laskov, C., Herzog, C., Lewandowski, J., and Hupfer, M.: Miniaturized photometrical methods for the rapid analysis of phosphate, ammonium, ferrous iron, and sulfate in pore water of freshwater sediments, Limnol. Oceanogr. Methods, 5, 63–71, https://doi.org/10.4319/lom.2007.5.63, 2007.

Lee, K., Kim, T.-W., Byrne, R. H., Millero, F. J., Feely, R. A., and Liu, Y.-M.: The universal ratio of boron to chlorinity for the North Pacific and North Atlantic oceans, Geochim. Cosmochim. Acta, 74, 1801–1811, https://doi.org/10.1016/j.gca.2009.12.027, 2010.

Liss, P. S., and Duce, R. A. (Eds.): The Sea Surface and Global Change, Cambridge University Press, ISBN 9780521562737, 1997.

Liss, P. S., and Merlivat, L.: Air–sea gas exchange rates: introduction and synthesis, in: The Role of Air–Sea Exchange in Geochemical Cycling, edited by: Buat-Ménard, P., Springer, Dordrecht, Netherlands, 113–127, https://doi.org/10.1007/978-94-009-4738-2_5, 1986.

Liu, J., Hrustić, E., Du, J., Gašparović, B., Čanković, M., Cukrov, N., Zhu, Z., and Zhang, R.: Net submarine groundwater-derived dissolved inorganic nutrients and carbon input to the oligotrophic stratified karstic estuary of the Krka River (Adriatic Sea, Croatia), J. Geophys. Res.-Oceans, 124, 4334–4349, https://doi.org/10.1029/2018JC014814, 2019.

Marcinek, S., Santinelli, C., Cindrić, A.-M., Evangelista, V., Gonnelli, M., Layglon, N., Mounier, S., Lenoble, V., and Omanović, D.: Dissolved organic matter dynamics in the pristine Krka River estuary (Croatia), Mar. Chem., 225, 103848, https://doi.org/10.1016/j.marchem.2020.103848, 2020.

Mehrbach, C., Culberson, C. H., Hawley, J. E., and Pytkowicx, R. M.: Measurement of the apparent dissociation constants of carbonic acid in seawater at atmospheric pressure 1, Limnol. Oceanogr., 18, 897–907, https://doi.org/10.4319/lo.1973.18.6.0897, 1973.

Milinković, A., Penezić, A., Kušan, A. C., Gluščić, V., Žužul, S., Skejić, S., Šantić, D., Godec, R., Pehnec, G., Omanović, D., Engel, A., and Frka, S.: Variabilities of biochemical properties of the sea surface

microlayer: Insights to the atmospheric deposition impacts, Sci. Total Environ., 838, 156440,
490 https://doi.org/10.1016/j.scitotenv.2022.156440, 2022.

Nimick, D. A., Gammons, C. H., and Parker, S. R.: Diel biogeochemical processes and their effect on the aqueous
chemistry of streams: A review, Chem. Geol., 283, 3–17, https://doi.org/10.1016/j.chemgeo.2010.08.017,
2011.

Perez, F. F., and Fraga, F.: Association constant of fluoride and hydrogen ions in seawater, Mar. Chem., 21, 161–
495 168, https://doi.org/10.1016/0304-4203(87)90036-3, 1987.

Poulson, S. R., and Sullivan, A. B.: Assessment of diel chemical and isotopic techniques to investigate
biogeochemical cycles in the upper Klamath River, Oregon, USA, Chem. Geol., 269, 3–11,
https://doi.org/10.1016/j.chemgeo.2009.05.016, 2010.

Ribas-Ribas, M., Battaglia, G., Humphreys, M. P., and Wurl, O.: Impact of nonzero intercept gas transfer velocity
500 parameterizations on global and regional ocean–atmosphere CO_2 fluxes, Geosciences, 9, 230,
https://doi.org/10.3390/geosciences9050230, 2019.

Ribas-Ribas, M., Hamizah Mustaffa, N. I., Rahlff, J., Stolle, C., and Wurl, O.: Sea Surface Scanner (S3): A
catamaran for high-resolution measurements of biogeochemical properties of the sea surface microlayer,
J. Atmos. Oceanic Technol., 34, 1433–1448, https://doi.org/10.1175/JTECH-D-17-0017.1, 2017.

505 Robinson, A. R., and Golnaraghi, M.: The Physical and Dynamical Oceanography of the Mediterranean Sea, in:
Ocean Processes in Climate Dynamics: Global and Mediterranean Examples, edited by: Malanotte-
Rizzoli, P. and Robinson, A. R., Springer Netherlands, 255–306, https://doi.org/10.1007/978-94-011-
0870-6_12, 1994.

Schneider, A., Tanhua, T., Körtzinger, A., and Wallace, D. W. R.: High anthropogenic carbon content in the eastern
510 Mediterranean, J. Geophys. Res.: Oceans, 115, C12, https://doi.org/10.1029/2010JC006171, 2010.

Sharp, J. D., Pierrot, D., Humphreys, M. P., Epitalon, J.-M., Orr, J. C., Lewis, E. R., and Wallace, D. W. R.:
CO2SYSv3 for MATLAB (v3.1), Zenodo [code], https://doi.org/10.5281/ZENODO.4023039, 2020.

Stolle, C., Ribas-Ribas, M., Badewien, T. H., Barnes, J., Carpenter, L. J., Chance, R., Damgaard, L. R., Durán
Quesada, A. M., Engel, A., Frka, S., Galgani, L., Gašparović, B., Gerriets, M., Hamizah Mustaffa, N. I.,
515 Herrmann, H., Kallajoki, L., Pereira, R., Radach, F., Revsbech, N. P., … and Wurl, O.: The MILAN
Campaign: Studying Diel Light Effects on the Air–Sea Interface, Bull. Amer. Meteor. Soc., 101, E146–
E166, https://doi.org/10.1175/BAMS-D-17-0329.1, 2020.

Takahashi, T., Sutherland, S. C., Chipman, D. W., Goddard, J. G., Ho, C., Newberger, T., Sweeney, C., and Munro, D. R.: Climatological distributions of pH, pCO$_2$, total CO$_2$, alkalinity, and CaCO$_3$ saturation in the global surface ocean, and temporal changes at selected locations, Mar. Chem., 164, 95–125, https://doi.org/10.1016/j.marchem.2014.06.004, 2014.

Takahashi, T., Sutherland, S. C., Sweeney, C., Poisson, A., Metzl, N., Tilbrook, B., Bates, N., Wanninkhof, R., Feely, R. A., Sabine, C., Olafsson, J., and Nojiri, Y.: Global sea–air CO$_2$ flux based on climatological surface ocean pCO2, and seasonal biological and temperature effects, Deep Sea Res. Part II: Topical Stud. Oceanogr., 49(9–10), 1601–1622, https://doi.org/10.1016/S0967-0645(02)00003-6, 2002.

Van Heuven, S., Pierrot, D., Rae, J. W. B., Lewis, E., and Wallace, D. W. R.: MATLAB Program Developed for CO$_2$ System Calculations, [software], https://doi.org/10.3334/cdiac/otg.co2sys_matlab_v1.1, 2011.

Wanninkhof, R.: Relationship between wind speed and gas exchange over the ocean revisited, Limnol. Oceanogr.: Methods, 12(6), 351–362, https://doi.org/10.4319/lom.2014.12.351, 2014.

Wong, P. P., Losada, I. J., Gattuso, J.-P., Hinkel, J., Khattabi, A., McInnes, K. L., Saito, Y., & Sallenger, A.: Coastal systems and low-lying areas, in: Climate Change 2014: Impacts, Adaptation, and Vulnerability. Part A: Global and Sectoral Aspects, edited by: Field, C. B., Barros, V. R., Dokken, D. J., Mach, K. J., Mastrandrea, M. D., Bilir, T. E., Chatterjee, M., Ebi, K. L., Estrada, Y. O., Genova, R. C., Girma, B., Kissel, E. S., Levy, A. N., MacCracken, A. N., Mastrandrea, P. R., White, L. L., Cambridge University Press, 361–409, https://doi.org/10.1017/CBO9781107415379.010, 2014.

Wurl, O., Landing, W. M., Mustaffa, N. I. H., Ribas-Ribas, M., Witte, C. R., & Zappa, C. J.: The Ocean's Skin Layer in the Tropics, in: Journal of Geophysical Research: Oceans, 124(1), 59–74, https://doi.org/10.1029/2018JC014021, 2019.

Wurl, O., Wurl, E., Miller, L., Johnson, K., & Vagle, S.: Formation and global distribution of sea-surface microlayers, in: Biogeosciences, 8(1), 121–135, https://doi.org/10.5194/bg-8-121-2011, 2011.

Zeebe, R. E., and Wolf-Gladrow, D. A.: CO$_2$ in Seawater: Equilibrium, Kinetics, Isotopes, Elsevier Oceanography Series, Vol. 65, Elsevier, Amsterdam, ISBN 0444509461, 2001.

520

525

530

535

540

545